Smart Design of Phenanthrene-Based Organic Photovoltaics Using Machine Learning

Hussein A.K. Kyhoiesh[1*], Azal S. Waheeb[2], Mustafa Al-Khafaji[3], Ashraf Y. Elnaggar[4], Islam H. El Azab[4], Mohamed H.H. Mahmoud[5], Mohammed F. Odhaib[6], Zainab A. Abass[7]

[1]*National University of Science and Technology, Nasiriyah, Dhi Qar, 64001, Iraq*

[2]*Department of Chemistry, College of Science, Al-Muthanna University, AL-Muthanna, Iraq*

[3]*College of Medical and Health Technologies, Al-Zahraa University for Women, Karbala, Iraq*

[4]*Department of Food Sciences and Nutrition, College of Science, Taif University, P.O. Box 11099, Taif 21944, Saudi Arabia*

[5]*Department of Chemistry, College of Science, Taif University, P.O. Box 11099, Taif 21944, Saudi Arabia*

[6]*Mazaya University College, Al-Zaytoun Street, Nasiriyah, Dhi-Qar, 64001, Iraq*

[7]*Optical Techniques Department, College of Health and Medical Techniques, Al-Mustaqbal University, 51001, Babylon, Iraq*

***Corresponding Author:** E-mail address: hussein.k.sultan@nust.edu.iq (H.A.K. Kyhoiesh); phone; (+964)7807229491; https://orcid.org/0000-0001-9705-9196

Methodlogy (Supplementary)

The DFT can be immensely helpful in designing new materials for OPVs.[1] It allows researchers to investigate the electronic structure and properties of materials at the molecular level, providing insights into their charge transport and optical properties.[2] By using DFT calculations, scientists can predict the behavior of potential HTMs, such as their energy levels, charge mobility, and absorption spectra.[3] This information guides the design and optimization of materials tailored for improved performance in OPV devices.[4]

All the proposed chemical structures were drawn by using ChemDraw software and were converted into their mol. Extension files. The files were optimized to their ground state energies by using Gaussian 09.5 (D.01) software[5] by utilizing CAM-B3LYP level of theory with 6-31G+(d,p).[6] To compute their UV-vis spectra, the resulting output file from the previous step was utilized for their TDFT calculations. For all the calculations, integral equation formalism-Polarizable Continuum Model (IEF-PCM) model with acetonitrile was used. We utilized complementary software tools such as GaussView,[7] ChemCraft to view the optimized geometries and their parameters respectively. Similarly, the GaussSum[8] software was employed to view the TDDFT spectra and its important parameters. Further computations and analyses were carried out using Multiwfn (v 3.6)[9] to facilitate the calculation of their Transition Density Matrix (TDM), Electron-Hole-Overlap and Density of State (DOS) related information.[10] A benchmarking study was previously conducted to compare results from various long-range and range-separated DFT levels and TD-CAM-B3LYP approach was chosen for its proven accuracy in predicting molecular excitation features,[11] especially in systems with significant charge transfer and low-lying excited states.[6]

In order to assess a molecule's responsiveness, global reactivity parameters, or GRPs, are commonly computed using Koopman's theorem. The conduct of the molecule may be understood with the aid of these factors, which include ionization potential (IP), electron affinity (EA), electronegativity (x), chemical potential (μ), hardness (η), softness (σ), and electrophilicity index (ω). To determine these parameters, Koopmans' theorem is frequently employed. The electron affinity (EA) is regarded as equal to the lowest unoccupied molecular orbital energy (E_{LUMO}),

while the IP is calculated as the negative of the highest occupied molecular orbital energy (E_{HOMO}). Equation 6-11 enables scientists to forecast a molecule's reactivity in a range of chemical reactions. To evaluate a molecule towards its chemical reactivity, global reactivity parameters (GRPs) are often calculated using Koopman's theorem.[12] These factors, including ionization potential (IP), electron affinity (EA), electronegativity (χ), chemical potential (μ), hardness (η), softness (σ), and electrophilicity index (ω), help in understanding the behavior of the molecule. Koopman's theorem is commonly used to determine these parameters.[12] Equation 6-11 allows scientists to predict a molecule's reactivity in various chemical reactions.

$$IP = -E_{HOMO} \quad \text{(Eq. 6)}$$

$$EA = -E_{LUMO} \quad \text{(Eq. 7)}$$

$$\chi = \left(\frac{IP + EA}{2}\right) \quad \text{(Eq. 8)}$$

$$\eta = \frac{1}{2}(E_{LUMO} - E_{HOMO}) \quad \text{(Eq. 9)}$$

$$\mu = -\chi \quad \text{(Eq. 10)}$$

$$\sigma = \frac{1}{2\eta} \quad \text{(Eq. 11)}$$

Pearson introduced the concept of ω as a counterpart to the concept of nucleophilicity.[13] The ω represents the tendency of a molecule or species to accept electrons and engage in electrophilic reactions. This parameter provides valuable information about the behaviour and reactivity of molecules in different chemical reactions (Eq. 12).

$$\omega = \frac{\mu^2}{2\eta} \quad \text{(Eq. 12)}$$

As the stabilization energy rises, the impact of donor capacities interacting becomes more pronounced,[14] as detailed in the equation (Eq. 13). The equation illustrates the increasing significance of the interaction between donor capabilities as the stabilization energy increases.

$$E^{(2)} = q_i \frac{(F_{i,j})^2}{\varepsilon_j - \varepsilon_i} \qquad (Eq.13)$$

The $E^{(2)}$ value is a significant indicator of stability energy. The NBO Fock matrix considers off-diagonal elements as $f_{i,j}$, with i and j denoting the diagonal values. The variable q_i reflects the orbital susceptibility of the donor.[15]

The open circuit voltage (V_{oc}) is the highest potential difference attainable by the cell in the absence of current flow.[16] In organic photovoltaics (OPVs), this value typically ranges from 0.5 to 1.2 eV.[17] In the present investigation, our aim was to determine this voltage using the formula provided (Eq 1).

$$V_{oc} = \frac{1}{e}([E_{HOMO}(D) - E_{LUMO}(A)]) - 0.03 \qquad \text{(Eq 1)}$$

Equation 2 illustrates how the light harvesting efficiency (LHE) was calculated.

$$LHE = 1 - 10^{-f} \qquad \text{(Eq 2)}$$

For a cell to passivate surface with uniform generation, its short-circuit current density (J_{sc}) is approximated by the following equation:

$$J_{SC} = qG(L_n + L_p)$$

where G is meant for generation rate while L_n and L_p being the electron and hole diffusion lengths.

The short circuit current, I_{SC}, is the short circuit current density, J_{SC}, times the cell area:

$$I_{SC} = J_{SC}A$$

The J_{sc} and V_{oc} being the maximum current and voltage respectively operate points when the power from the solar cell is zero. So, the fill factor (FF) determines the maximum power of a solar cell. It is defined by its ratio of the maximum power from the solar cell to the product of V_{oc} and I_{sc} so that:

$$FF = \frac{P_{MP}}{V_{OC} \times I_{SC}}$$

$$FF = \frac{V_{MP} I_{MP}}{V_{OC} I_{SC}}$$

References

1. Szlapa-Kula A, Ledwon P, Krawiec A, Kula S (2023) Dibenzofulvene Derivatives as Promising Materials for Photovoltaic and Organic Electronics. Energies 16:8027. https://doi.org/10.3390/en16248027

2. Kumar V, Koudjina S, Verma P, Chetti P (2023) Optoelectronic design and charge transport properties of Benzodifuran (BDF) isomers for organic electronic devices: DFT/TD-DFT insights. Spectrochimica Acta Part A: Molecular and Biomolecular Spectroscopy 290:122266. https://doi.org/10.1016/j.saa.2022.122266

3. Chi W-J, Sun P-P, Li Z-S (2016) How to regulate energy levels and hole mobility of spiro-type hole transport materials in perovskite solar cells. Phys Chem Chem Phys 18:27073–27077. https://doi.org/10.1039/C6CP03316D

4. Yang C, Su C, Hu H, et al (2023) Performance optimization of photovoltaic and solar cells via a hybrid and efficient chimp algorithm. Solar Energy 253:343–359. https://doi.org/10.1016/j.solener.2023.02.036

5. Frisch JM, Trucks WG, Schlegel BH, others (2013) Gaussian 09, Revision D. 01, Gauss. Inc, Wallingford CT

6. Yanai T, Tew DP, Handy NC (2004) A new hybrid exchange--correlation functional using the Coulomb-attenuating method (CAM-B3LYP). Chemical physics letters 393:51–57

7. LI W, Xie H, Huang Y, et al (2016) Application of Gaussian 09/GaussView 5.0 in analytical chemistry teaching. Journal of Kunming Medical University 134–136

8. O'boyle NM, Tenderholt AL, Langner KM (2008) cclib: A library for package-independent computational chemistry algorithms. Journal of Computational Chemistry 29:839–845. https://doi.org/10.1002/jcc.20823

9. Lu T, Chen F (2012) Multiwfn: A multifunctional wavefunction analyzer. Journal of Computational Chemistry 33:580–592. https://doi.org/10.1002/jcc.22885

10. Zhao Y, Truhlar DG (2008) The M06 suite of density functionals for main group thermochemistry, thermochemical kinetics, noncovalent interactions, excited states, and transition elements: two new functionals and systematic testing of four M06-class functionals and 12 other functionals. Theor Chem Account 120:215–241. https://doi.org/10.1007/s00214-007-0310-x

11. Hassan AU, Li Y (2024) Convenient and facile theoretical design strategy to amplify NLO response of N-doped-indolo[3,2,1-jk]carbazole push–pull A-π-D-π-A switches. Journal of Chemical Technology & Biotechnology 99:355–369. https://doi.org/10.1002/jctb.7530

12. Luo J, Xue ZQ, Liu WM, et al (2006) Koopmans' theorem for large molecular systems within density functional theory. The Journal of Physical Chemistry A 110:12005–12009

13. Green DT, Pearson JM (2009) The Examination of Two Web Site Usability Instruments for Use in B2C E-Commerce Organizations. Journal of Computer Information Systems 49:19–32. https://doi.org/10.1080/08874417.2009.11645337

14. Jacob JM, Kurup MRP, Nisha K, et al (2020) Mixed ligand copper(II) chelates derived from an O, N, S- donor tridentate thiosemicarbazone: Synthesis, spectral aspects, FMO, and NBO analysis. Polyhedron 189:114736. https://doi.org/10.1016/j.poly.2020.114736

15. Silvi B, Savin A (1994) Classification of chemical bonds based on topological analysis of electron localization functions. Nature 371:683–686. https://doi.org/10.1038/371683a0

16. Du T, Kim J, Ngiam J, et al (2018) Elucidating the Origins of Subgap Tail States and Open-Circuit Voltage in Methylammonium Lead Triiodide Perovskite Solar Cells. Advanced Functional Materials 28:1801808

17. Sharma A, Masoumi S, Gedefaw D, et al (2022) Flexible solar and thermal energy conversion devices: Organic photovoltaics (OPVs), organic thermoelectric generators (OTEGs) and hybrid PV-TEG systems. Applied Materials Today 29:101614. https://doi.org/10.1016/j.apmt.2022.101614

```
[ ]: import psi4

# Set the memory and output options
psi4.set_memory('2 GB')
psi4.set_output_file('output.dat', False)

# Define the molecule
molecule = psi4.geometry("""
0 1
O 0.000000 0.000000 0.000000
H 0.000000 0.000000 1.000000
H 0.000000 1.000000 0.000000
""")

# Calculate the ground state energy using DFT
E_ground = psi4.energy('B3LYP/6-31G(d)', molecule=molecule)

# Calculate the excited state energy using TDDFT
E_excited = psi4.td_energy('B3LYP/6-31G(d)', nroots=1, molecule=molecule)

# Calculate the exciton binding energy
E_b = E_ground - E_excited

print(f"Exciton Binding Energy: {E_b} Hartree")
```

Fig. S1. Python code for calculating the exciton binding energies

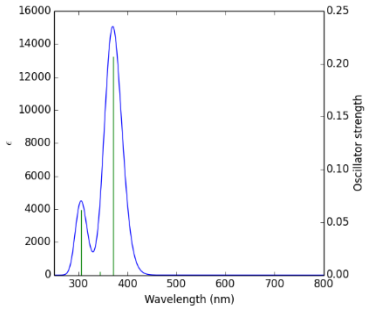
ϵ
Oscillator strength
Wavelength (nm)

1

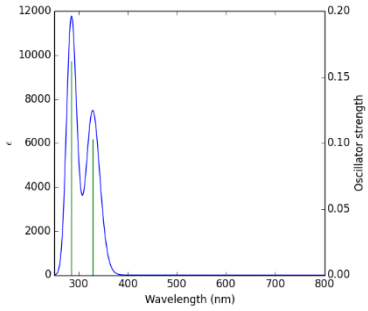
ϵ
Oscillator strength
Wavelength (nm)

2

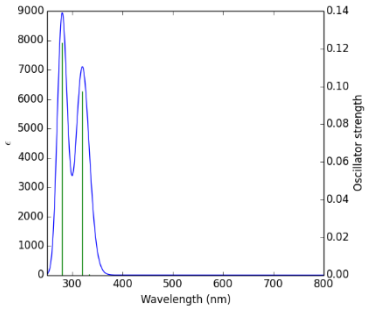
ϵ
Oscillator strength
Wavelength (nm)

3

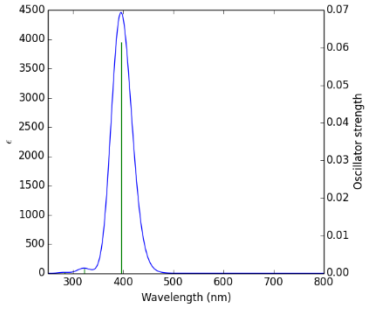
ϵ
Oscillator strength
Wavelength (nm)

4

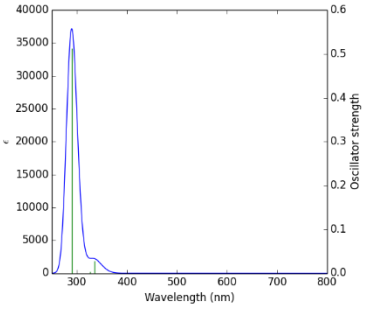
ϵ
Oscillator strength
Wavelength (nm)

5

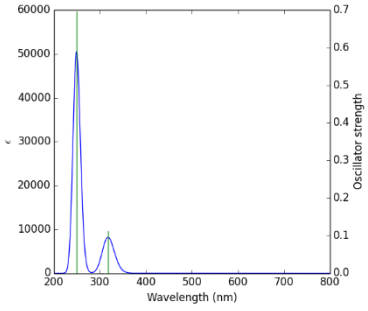
ϵ
Oscillator strength
Wavelength (nm)

6

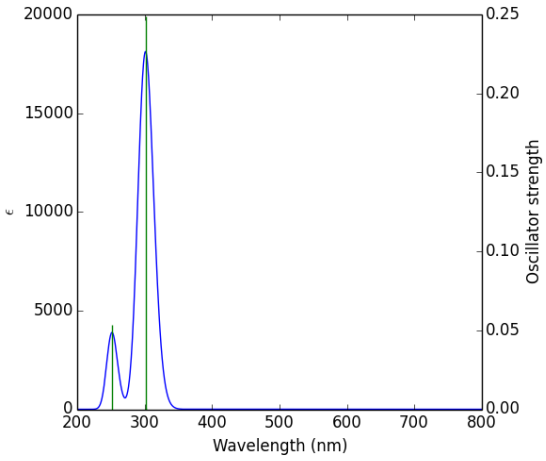
ϵ
Oscillator strength
Wavelength (nm)

7

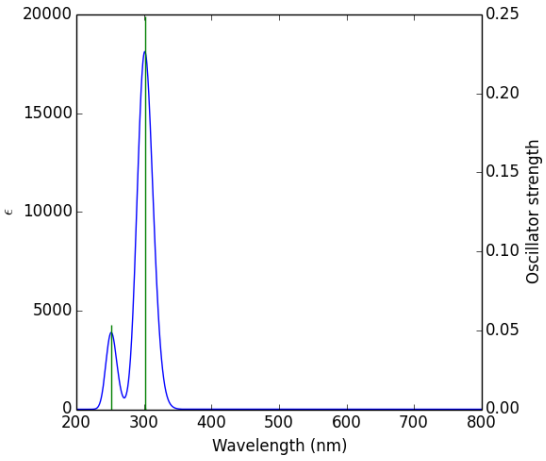
ϵ
Oscillator strength
Wavelength (nm)

8

Fig. S 2. TDDFT spectra of the selected organic dyes

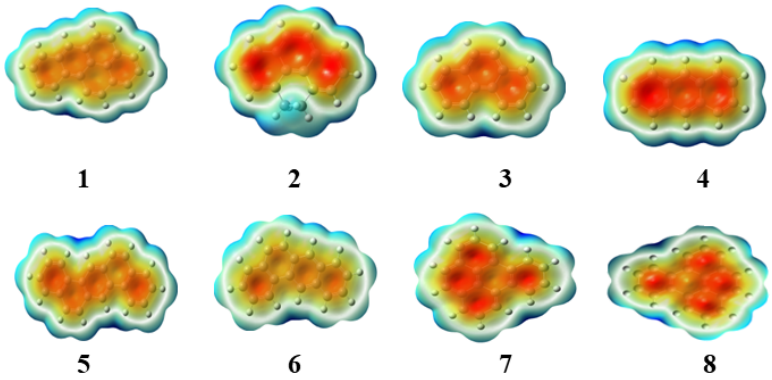

Fig. S 3. Molecular electrostatic potentials for the selected organic dyes

Optimized geometrical paramters of selected organic dyes

Center Number	Atomic Number	Atomic Type	Coordinates (Angstroms) X	Y	Z
1	6	0	10.417418	-10.528867	0.000000
2	6	0	11.199451	-9.215861	0.000000
3	6	0	8.884872	-10.461808	0.000000
4	6	0	10.412825	-7.899080	0.000000
5	6	0	8.255973	-9.253701	0.000000
6	6	0	9.051141	-7.919956	0.000000
7	6	0	11.069830	-11.718532	0.000000
8	6	0	12.610275	-11.737588	0.000000
9	6	0	12.554041	-9.227908	0.000000
10	6	0	13.291922	-10.570053	0.000000
11	6	0	13.383318	-13.071500	0.000000
12	6	0	14.742396	-13.065373	0.000000
13	6	0	14.814605	-10.563616	0.000000
14	6	0	15.504478	-11.724680	0.000000
15	6	0	13.356928	-7.905974	0.000000
16	6	0	15.541080	-9.215384	0.000000
17	6	0	14.725527	-7.900376	0.000000
18	6	0	16.896356	-9.184434	0.000000
19	6	0	17.043751	-11.694989	0.000000
20	6	0	17.695675	-10.504112	0.000000
21	1	0	8.309917	-11.364209	0.000000
22	1	0	10.933760	-6.964453	0.000000
23	1	0	7.186418	-9.222862	0.000000

24	1	0	8.515532	-6.993660	0.000000
25	1	0	10.518993	-12.635853	0.000000
26	1	0	12.851166	-13.999785	0.000000
27	1	0	15.282590	-13.989002	0.000000
28	1	0	12.830346	-6.974517	0.000000
29	1	0	15.243938	-6.964347	0.000000
30	1	0	17.410922	-8.246286	0.000000
31	1	0	17.598099	-12.610193	0.000000
32	1	0	18.765419	-10.480720	0.000000

Dye 2

Center Number	**Atomic Number**	**Atomic Type**	**Coordinates (Angstroms) X**	**Y**	**Z**
1	**6**	**0**	**12.458701**	**-10.836049**	**-1.035545**
2	**6**	**0**	**12.471996**	**-12.356217**	**-0.998644**
3	**6**	**0**	**11.295550**	**-10.165775**	**-0.972323**
4	**6**	**0**	**11.301455**	**-13.045467**	**-1.004561**
5	**6**	**0**	**9.973417**	**-10.914240**	**-1.037222**
6	**6**	**0**	**9.962711**	**-12.272466**	**-1.056574**
7	**6**	**0**	**13.784072**	**-10.087862**	**-1.166432**
8	**6**	**0**	**14.958230**	**-10.775420**	**-1.126662**
9	**6**	**0**	**13.834073**	**-13.062555**	**-0.963594**
10	**6**	**0**	**14.983459**	**-12.326367**	**-1.007274**
11	**6**	**0**	**11.278302**	**-8.646569**	**-0.813453**
12	**6**	**0**	**10.095780**	**-7.973509**	**-0.853402**
13	**6**	**0**	**8.680515**	**-10.088000**	**-1.070793**
14	**6**	**0**	**8.741911**	**-8.725516**	**-1.001212**
15	**6**	**0**	**12.611922**	**-7.911371**	**-0.570269**
16	**6**	**0**	**13.755447**	**-8.561089**	**-1.381701**

17	1	0	11.305618	-14.115133	-0.978145
18	1	0	9.034996	-12.803609	-1.102746
19	1	0	15.882246	-10.238720	-1.181852
20	1	0	13.883048	-14.129894	-0.906244
21	1	0	15.926477	-12.829958	-0.962406
22	1	0	10.097196	-6.906140	-0.778416
23	1	0	7.732711	-10.578616	-1.147370
24	1	0	7.834397	-8.160386	-1.045321
25	1	0	12.529271	-6.884648	-0.859939
26	1	0	12.833452	-7.974372	0.474650
27	1	0	14.682469	-8.124247	-1.073969
28	1	0	13.601177	-8.381506	-2.425181

Dye-3

Center Number	Atomic Number	Atomic Type	Coordinates (Angstroms) X	Y	Z
1	6	0	11.205181	-11.073522	-0.065078
2	6	0	11.206438	-12.599292	-0.093838
3	6	0	10.033360	-10.396844	-0.055695
4	6	0	10.036641	-13.285265	-0.110139
5	6	0	8.710969	-11.158260	-0.073857
6	6	0	8.701324	-12.514173	-0.099448
7	6	0	12.553327	-10.342412	-0.047408
8	6	0	13.713466	-11.055675	-0.057509
9	6	0	12.557658	-13.325332	-0.103629
10	6	0	13.715673	-12.608354	-0.086776
11	6	0	9.992978	-8.863914	-0.026908
12	6	0	8.795303	-8.215635	-0.018131

13	6	0	7.406733	-10.350880	-0.062390
14	6	0	7.449127	-8.989676	-0.036603
15	1	0	10.040259	-14.355069	-0.130297
16	1	0	7.772753	-13.045675	-0.112144
17	1	0	12.582343	-9.272997	-0.027164
18	1	0	14.647052	-10.533029	-0.044962
19	1	0	12.590506	-14.394640	-0.123690
20	1	0	14.650840	-13.128270	-0.093884
21	1	0	10.904903	-8.304343	-0.013733
22	1	0	8.781506	-7.145913	0.002001
23	1	0	6.463984	-10.856821	-0.074642
24	1	0	6.531377	-8.439607	-0.028876

Dye-4

Center Number	Atomic Number	Atomic Type	Coordinates (Angstroms) X	Y	Z
1	6	0	10.272856	-9.726469	-0.039045
2	6	0	10.270355	-11.253000	-0.046452
3	6	0	9.105831	-9.039570	-0.039397
4	6	0	9.101084	-11.936035	-0.053450
5	6	0	7.769515	-9.806986	-0.047331
6	6	0	7.767291	-11.164202	-0.053917
7	6	0	11.625264	-9.001281	-0.031260
8	6	0	12.779084	-9.723552	-0.031116
9	6	0	11.620378	-11.982658	-0.045724
10	6	0	12.776559	-11.264209	-0.038591
11	6	0	14.135643	-9.005365	-0.023350
12	6	0	15.292085	-9.722679	-0.023170

13	6	0	14.130757	-11.986880	-0.037814
14	6	0	15.289544	-11.273396	-0.030696
15	1	0	9.111542	-7.969598	-0.034192
16	1	0	9.103288	-13.006020	-0.058628
17	1	0	6.843926	-9.270157	-0.047651
18	1	0	6.839947	-11.697966	-0.059429
19	1	0	11.661145	-7.931896	-0.025963
20	1	0	11.652754	-13.052156	-0.050804
21	1	0	14.172159	-7.936001	-0.018054
22	1	0	16.227488	-9.203167	-0.017693
23	1	0	14.163768	-13.056358	-0.042893
24	1	0	16.223238	-11.795999	-0.030280

Dye-5

Center Number	Atomic Number	Atomic Type	Coordinates (Angstroms) X	Y	Z
1	6	0	10.259664	-10.580638	-0.056663
2	6	0	10.257125	-12.106088	-0.059972
3	6	0	8.910976	-9.850449	-0.046659
4	6	0	8.906182	-12.833140	-0.053134
5	6	0	7.750881	-10.563384	-0.040979
6	6	0	7.747030	-12.116136	-0.044344
7	6	0	11.428910	-9.897335	-0.062466
8	6	0	12.762746	-10.668744	-0.072466
9	6	0	11.424366	-12.792849	-0.068748
10	6	0	12.760611	-12.025513	-0.075409
11	6	0	14.097622	-9.901063	-0.079115
12	6	0	15.270050	-10.580904	-0.087911

13	6	0	14.093086	-12.797320	-0.085402
14	6	0	15.267634	-12.121110	-0.091254
15	6	0	14.100390	-8.361078	-0.075773
16	6	0	15.275226	-7.685602	-0.081624
17	6	0	16.605053	-9.813211	-0.094561
18	6	0	16.607477	-8.458007	-0.091620
19	6	0	8.864532	-14.372464	-0.056232
20	6	0	7.674382	-15.018512	-0.050220
21	6	0	6.396779	-12.858720	-0.037548
22	6	0	6.362560	-14.213593	-0.040288
23	1	0	8.881659	-8.780854	-0.044146
24	1	0	6.817649	-10.040000	-0.034016
25	1	0	11.426498	-8.827340	-0.060122
26	1	0	11.418711	-13.862831	-0.071043
27	1	0	14.091668	-13.867316	-0.087724
28	1	0	16.193510	-12.657398	-0.098197
29	1	0	13.174730	-7.824418	-0.068829
30	1	0	15.277171	-6.615606	-0.079299
31	1	0	17.530735	-10.349833	-0.101504
32	1	0	17.535070	-7.924668	-0.096239
33	1	0	9.776564	-14.931973	-0.063138
34	1	0	7.646005	-16.088134	-0.052375
35	1	0	5.482713	-12.302539	-0.030640
36	1	0	5.422334	-14.724331	-0.035542

Dye-6

Center Number	Atomic Number	Atomic Type	Coordinates (Angstroms) X	Y	Z

1	6	0	9.777800	-11.064900	-0.028200
2	6	0	9.793200	-12.453900	-0.028000
3	6	0	8.572100	-10.381800	-0.022000
4	6	0	8.596500	-13.156000	-0.019600
5	6	0	7.378300	-11.083200	-0.010500
6	6	0	7.391100	-12.469100	-0.008700
7	6	0	10.966200	-10.354200	-0.032200
8	6	0	12.190500	-11.019500	-0.038400
9	6	0	11.004400	-13.125000	-0.034000
10	6	0	12.196200	-12.415400	-0.039600
11	6	0	13.406600	-10.328000	-0.041800
12	6	0	14.603800	-11.043800	-0.045800
13	6	0	13.394700	-13.110700	-0.048300
14	6	0	14.597400	-12.426700	-0.051900
15	6	0	13.462500	-8.935700	-0.042300
16	6	0	14.681800	-8.278800	-0.039600
17	6	0	15.821400	-10.383900	-0.038800
18	6	0	15.862500	-9.000400	-0.035000
19	1	0	8.563900	-9.270100	-0.024100
20	1	0	8.602400	-14.266100	-0.019700
21	1	0	6.411800	-10.535300	-0.000700
22	1	0	6.432400	-13.030300	0.000000
23	1	0	10.922300	-9.247400	-0.030100
24	1	0	11.023700	-14.237400	-0.035200
25	1	0	13.393500	-14.222000	-0.049400
26	1	0	15.558400	-12.985500	-0.058700
27	1	0	12.535700	-8.328700	-0.042800
28	1	0	14.711200	-7.168200	-0.039300
29	1	0	16.769300	-10.966300	-0.036000

30	1	0	16.840100	-8.470000	-0.028800

Dye-7

Center Number	Atomic Number	Atomic Type	Coordinates (Angstroms) X	Y	Z
1	6	0	10.178178	-12.690858	-0.050633
2	6	0	10.189945	-14.213150	-0.042971
3	6	0	9.012794	-12.020307	-0.047514
4	6	0	9.020838	-14.903425	-0.032922
5	6	0	7.690819	-12.775177	-0.036283
6	6	0	7.681606	-14.132844	-0.029338
7	6	0	11.509036	-11.939084	-0.061896
8	6	0	12.679599	-12.634818	-0.064916
9	6	0	11.549890	-14.923388	-0.046975
10	6	0	12.700277	-14.189715	-0.057135
11	6	0	8.993885	-10.491890	-0.055166
12	6	0	7.804127	-9.829517	-0.051871
13	6	0	6.393347	-11.956362	-0.033178
14	6	0	6.449487	-10.593069	-0.040415
15	6	0	10.328421	-9.717907	-0.066564
16	6	0	11.507480	-10.396326	-0.069718
17	6	0	10.327308	-8.178153	-0.074372
18	6	0	11.500732	-7.499804	-0.084378
19	6	0	12.839196	-9.623469	-0.081092
20	6	0	12.835931	-8.268064	-0.087949
21	1	0	9.026865	-15.973395	-0.027520
22	1	0	6.753561	-14.665357	-0.021440
23	1	0	13.606056	-12.099547	-0.072820

24	1	0	11.596138	-15.992376	-0.041806
25	1	0	13.641891	-14.697905	-0.059822
26	1	0	7.801283	-8.759535	-0.057287
27	1	0	5.445937	-12.453608	-0.025350
28	1	0	5.536927	-10.034384	-0.038146
29	1	0	9.400328	-7.643736	-0.071898
30	1	0	11.499624	-6.429818	-0.089798
31	1	0	13.767077	-10.156322	-0.083580
32	1	0	13.761518	-7.731290	-0.095848

Dye 8

Center Number	Atomic Number	Atomic Type	Coordinates (Angstroms) X	Y	Z
1	6	0	-0.947777	-0.672266	-0.000002
2	6	0	-2.261405	-1.441652	-0.000001
3	6	0	-0.947777	0.672266	-0.000001
4	6	0	-3.442802	-0.772552	0.000002
5	6	0	-2.261405	1.441652	0.000001
6	6	0	-3.442802	0.772553	0.000003
7	6	0	0.367597	-1.450897	-0.000002
8	6	0	0.348352	-2.812477	-0.000003
9	6	0	-2.198770	-2.974616	0.000000
10	6	0	-0.989093	-3.605847	0.000001
11	6	0	0.367597	1.450897	-0.000001
12	6	0	0.348352	2.812477	-0.000001
13	6	0	-2.198770	2.974616	0.000001
14	6	0	-0.989093	3.605847	-0.000002
15	6	0	1.704056	0.680155	-0.000002

16	**6**	**0**	**1.704056**	**-0.680155**	**-0.000002**
17	**6**	**0**	**3.038133**	**1.449014**	**0.000000**
18	**6**	**0**	**4.211346**	**0.770226**	**0.000003**
19	**6**	**0**	**3.038133**	**-1.449014**	**0.000000**
20	**6**	**0**	**4.211346**	**-0.770226**	**0.000003**
21	**1**	**0**	**-4.367226**	**-1.311384**	**0.000007**
22	**1**	**0**	**-4.367226**	**1.311384**	**0.000004**
23	**1**	**0**	**1.274375**	**-3.348556**	**-0.000006**
24	**1**	**0**	**-3.102284**	**-3.547820**	**0.000002**
25	**1**	**0**	**-0.959963**	**-4.675450**	**0.000004**
26	**1**	**0**	**1.274375**	**3.348556**	**-0.000002**
27	**1**	**0**	**-3.102284**	**3.547820**	**0.000003**
28	**1**	**0**	**-0.959963**	**4.675450**	**-0.000004**
29	**1**	**0**	**3.039035**	**2.519014**	**-0.000002**
30	**1**	**0**	**5.138238**	**1.304802**	**0.000008**
31	**1**	**0**	**3.039035**	**-2.519014**	**-0.000001**
32	**1**	**0**	**5.138238**	**-1.304802**	**0.000008**

Table S1. Global chemical reactivity parameters of selected organic dyes

Comp.	E_H	E_L	ΔE_{H-L}	IP	EA	χ	μ	η	S	ω
V	-5.616	-1.971	*3.65*	5.62	1.97	3.79	-3.79	1.82	0.27	3.95
1	-5.778	-1.6119	*4.17*	5.78	1.61	3.69	-3.69	2.08	0.24	3.28
2	-5.859	-1.593	*4.27*	5.86	1.59	3.73	-3.73	2.13	0.23	3.25
3	-5.481	-2.025	*3.46*	5.48	2.03	3.75	-3.75	1.73	0.29	4.08
4	-5.832	-1.728	*4.10*	5.83	1.73	3.78	-3.78	2.05	0.24	3.48
5	-3.51	0.432	*3.94*	3.51	-0.43	1.54	-1.54	1.97	0.25	0.60
6	-3.618	0.4914	*4.11*	3.62	-0.49	1.56	-1.56	2.05	0.24	0.59
7	-4.347	4.914	*9.26*	4.35	-4.91	-0.28	0.28	4.63	0.11	0.01